CHEMISTRY
A EUROPEAN JOURNAL

FULL PAPER

DOI: 10.1002/chem.201202498

Molecular Daisy Chains: Synthesis and Aggregation Studies of an Amphiphilic Molecular Rod

Jürgen Rotzler,[a] Sylvie Drayss,[a] Oliver Hampe,[b] Daniel Häussinger,[a] and Marcel Mayor*[a, b]

Dedicated to Professor François Diedrich on the occasion of his 60th birthday

Abstract: A water-soluble cyclophane as the loop subunit, monofunctionalized with a molecular rod, has been synthesized to introduce a new binding motif for mechanically interlinked oligomers. It has been demonstrated that this hermaphroditic compound forms [c2]daisy chains in polar solvent over a wide range of concentrations. Furthermore, evidence for the formation of higher mechanically interlinked oligomers above the critical aggregation concentration has been obtained.

Keywords: amphiphiles · cyclophanes · daisy chains · host–guest chemistry · self-assembly

Introduction

One of the main targets of materials science is the conversion of macroscopic physical phenomena into altered and tailored phenomena with a specific physical output. Therefore the macroscopic input has to induce a change in the investigated material on the microscopic level, which then provides the desired physical output. Such changes in the molecular dimension can be of a structural,[1] conformational,[2–7] electrochemical,[8] or photochemical[9,10] nature or in the intermolecular arrangement of the molecules.[11–13] Current research in surface and polymer science is thus focused on the development of new potential structures that are able to fulfill the desired needs of providing, for example, more scratch-resistant lacquers and plastics,[14] conducting plastics,[15,16] or self-cleaning surfaces,[17] to name just a few. One of the major drawbacks in polymer science is that for each different purpose a completely new macromolecule has to be synthesized starting from increasingly complex monomers. To overcome this time-consuming and challenging problem, a new concept for generating tailored polymers has been put forward over the last two decades[18–20] by using the tremendous findings in supramolecular chemistry[21–24] starting with the demonstration by Pedersen in 1967 that host–guest complexation is not limited to natural systems with synthetic crown ethers.[25] By using secondary interactions (hydrogen bonding, hydrophobic effects, π–π stacking, or van der Waals' interactions) to assemble oligomeric or polymeric structures, covalent irreversible bonding in macromolecules is replaced by mechanical bonding, which gives rise to several advantages.[26,27] One is the reversibility of these dynamic aggregates, which makes them thermodynamically controlled regimes. This in turn can lead to self-healing as incorrect chain extensions can be reversed as the system strives for energy minimization.[28] Furthermore, the thermodynamic control of chain propagation allows precise chemical engineering on a supramolecular scale by changing the external conditions used for the propagation reaction.[20,27,28] As a positive side effect, only monomers have to be synthesized. Studying and understanding the aggregation behavior allows appropriate reaction conditions to be developed to enable the formation of various architectural devices.[29,30] Moreover, such systems are extremely sensitive to the external environment (e.g., mechanical stress or heat) because of possible internal movement that not only affects the degree of polymerization but also alters the bulk properties of these macromolecular assemblies, such as the viscosity, dimensions, and rheology.[27,31] This approach makes designed architectures of mechanically interlocked molecules (MIM) possible, leading to new solid-state electronic devices, mechanized nanoparticles, nanoelectromechanical systems, switches, molecular motors and machines, as well as nanovalves and molecular actuators.[27] Various recognition motifs were introduced to achieve such daisy-chain-like polymers.[26] Dibenzo[24]crown-8 and dibenzylammonium salts,[20,28,32,33] viologen,[20] or 1,2-bis(pyridinium)ethane[29] binding have been widely used, as well as cyclobis(paraquat-*p*-phenylene)–naphthyl or TTF[27] and cyclodextrin–naphthyl.[34,35] Nevertheless, the assembly of the synthetically challenging monomers often yielded only [c2]daisy chains or required a multistep assembly to achieve the desired macromolecules of higher order. In some cases the dimeric [c2]daisy chain was the synthetic target of the studies, but to

[a] Dr. J. Rotzler, S. Drayss, Dr. D. Häussinger, Prof. Dr. M. Mayor
Department of Chemistry, University of Basel
St. Johanns-Ring 19, 4056 Basel (Switzerland)
Fax: (+41) 61-267-10-16
E-mail: marcel.mayor@unibas.ch

[b] Dr. O. Hampe, Prof. Dr. M. Mayor
Institute of Nanotechnology, Karlsruhe Institute of Technology (KIT)
P.O. Box 3640, 76021 Karlsruhe (Germany)

Supporting information for this article is available on the WWW under http://dx.doi.org/10.1002/chem.201202498.

make them sufficiently stable they had to be stoppered after assembly.[26] Furthermore, in all cases a photo- or electrochemical input was used to generate internal motion. None of the examples in the literature feature a structural motif that allows altering of the physical output by internal motion. Therefore we report herein an inversed recognition motif for which the complexation behavior of neutral aromatic compounds with Diederich-type cyclophanes was used.[36,37] In this case the driving force for assembly is the nonclassical hydrophobic effect, which allows complexation in polar solvents like water or alcohols. In this project it was of interest to discover how such oligophenylene-ethynylene molecules (OPE) comprising a terminal loop aggregate in water and if different daisy chains can be observed by just varying the concentration. If a defined assembly could be obtained, it would then be of interest to functionalize the monomers such that by a simple reaction higher oligomers can be synthesized resulting in a higher control of the molecular architecture. Moreover, the inversed binding motif in principle allows alteration of physical outputs by applying mechanical stress, in stark contrast to the systems known to date for which altering the internal motion was the initial aim.

In this paper we report the synthesis and self-aggregation studies of monomer **1** (Figure 1) to provide a platform for future investigations on mechanically bonded oligomers or even polymers. The design of target compound **1** profits to a large extent from the outstanding work of Diederich and co-workers.[36–40] Similarly to this proceeding work, two diphenylmethane units function as rigid spacers and cavity walls. Water solubility of the cyclophane is achieved by the introduction of quaternary amines; by varying the counter ions the solubility can be fine-tuned. Furthermore, these positively charged moieties support, together with steric repulsion, the opening and flattening of the cavity loop by electrostatic repulsion. From solid-state structures it is known that the quaternary amines are located at a distance from the cavity and that the oxygen atoms face outwards, away from the cavity, making it hydrophobic, a necessity for the final supramolecular assembly.[36] The size of the cavity is defined by the length of the interlinking alkane chains between the two diphenylmethane units. In accord with the studies of Diederich et al., a propane chain was chosen, which gives a cavity large enough to complex benzene cores.[36] Molecular complexation of neutral substituted benzene guests in aqueous solution is driven by a strong nonclassical hydrophobic effect.[37] Therefore, a hydrophobic oligophenylene-ethynylene rod is linked to the monofunctionalized cyclophane through a benzyl group, which gives the host system further flexibility and hence allows for a perfect, thermodynamic-driven binding of the guest.

In addition, it is well known that the nature of the pivot heteroatom can dramatically influence the aggregation behavior of the hermaphroditic daisy-chain monomer, thus allowing for further tuning of the system by changing the bonding angle of the OPE with respect to the normal of the mean plane.[41] The free rotation around the phenolic and

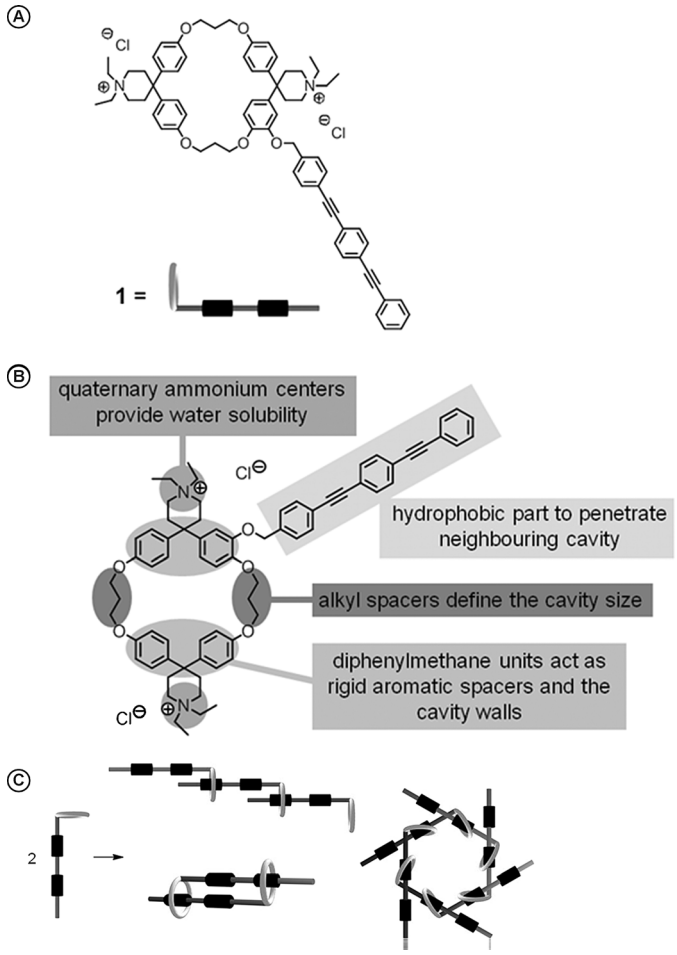

Figure 1. A) Hermaphroditic monomer **1** with inversed recognition motif. B) Structure–property relationship of the target amphiphile **1**. C) Possible aggregates formed in polar solvents.

benzylic bonds of the Ar–O–CH_2–OPE motif allows the guest to find an ideal spatial arrangement with respect to the mean plane of the host, which is crucial for the formation of various daisy-chain-like aggregates. A 90° angle between host and guest, which is only accessible because of the benzylic linkage, would maybe be an ideal arrangement to obtain perfect inclusion of the host. Furthermore, this flexibility allows for conformations in which, for example, the host is placed in front of the cavity like a cap (even self-threading cannot be excluded) and therefore potentially "blocks" one side of the cavity leading to linear acyclic rather than cyclic daisy chains.

Results and Discussion

Synthesis: The assembly of the loop subunit profits to a large extent from the cyclophane chemistry developed by Diederich and co-workers,[38–40] whereas the formation of the rigid molecular rod is based on classical Sonogashira coupling chemistry.[42] The oligophenylene-ethynylene unit is

considered to be coupled to the cyclophane at a late stage in the synthesis, which allows alteration of the length and substitution pattern of the molecular rod to be altered and thus optimization of the extent of intermolecular stacking.

As already mentioned, the amphiphilic monomer **1** was synthesized inspired by the numerous synthetic routes towards monofunctionalized Diederich-type water-soluble cyclophanes reported in literature.[36–40] Molecules **2** and **3** were synthesized according to the literature[40] by Grignard reaction of 4-bromoanisole and *N*-acetylpiperidin-4-one followed by elimination of the resulting tertiary alcohol **2** and deprotection of the methoxy group in one step using strong Lewis acidic boron tribromide (Scheme 1). Because for the purification of the resulting phenol only washing of the crude with water and diethyl ether was required, the reaction protocol could be applied to a larger-scale synthesis (25 g starting material) from which an overall yield of 63% was obtained. In the following step, the free phenolic hydroxy group was protected with a photocleavable 2-nitrobenzyl group in a yield of 79%, a reaction that was necessary because a stepwise cyclization protocol was chosen for the cyclophane assembly.[39] Then the cavity wall bearing the monofunctionalization was introduced by addition of 2-methoxyphenol (guaiacol) to the styrene double bond of **4** in strong Lewis acidic media using a large excess of boron trifluoride (Scheme 1).[40] The addition of guaiacol seems to be reversible leading to the electronically and thermodynamically favored coupled product *para* to the hydroxy group after stirring for 9 days at room temperature (99%). Shorter reaction times led to the formation of regioisomers.

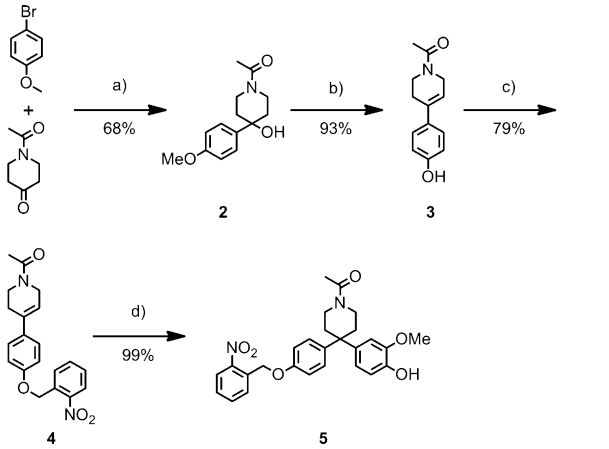

Scheme 1. Synthesis of the functionalized cyclophane component **5**. Reagents and conditions: a) Mg, THF, reflux, 1.5 h, then *N*-acetylpiperidin-4-one, THF, RT, 4 h; b) BBr_3, CH_2Cl_2, reflux, 3 h; c) 2-nitrobenzyl chloride, K_2CO_3, MeCN, reflux, 6.5 h; d) 2-methoxyphenol, $BF_3{\cdot}OEt_2$, CH_2Cl_2, RT, 9 d.

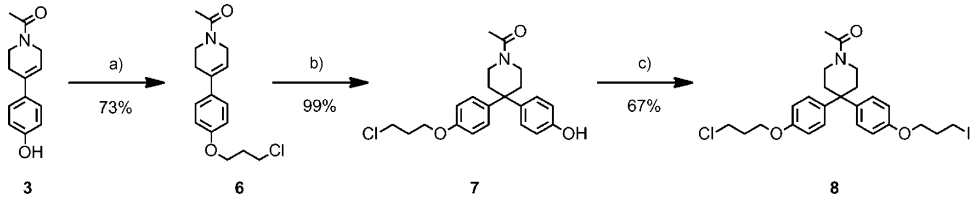

Scheme 2. Synthesis of the unfunctionalized cyclophane component **8**. Reagents and conditions: a) 1,3-dichloropropane, K_2CO_3, MeCN, reflux, 26 h; b) phenol, $BF_3{\cdot}OEt_2$, CH_2Cl_2, RT, 23 h; c) 1,3-diiodopropane, BHT, K_2CO_3, acetone, reflux, 5 h.

The symmetrical unit **8** of the cyclophane was synthesized starting from phenol **3** by the introduction of 1,3-dichloropropane through an S_N2 reaction, followed by the addition of phenol to the obtained alkene to give a yield of 99% after column chromatography and recrystallization from acetonitrile. To avoid homocoupling of the symmetrical diphenylpiperidine moiety **8**, the second alkyl spacer of cyclophane **11** was installed at the remaining free hydroxy group of **7**. Therefore phenol **7** was treated with 1,3-diiodopropane in the presence of radical inhibitor 3,5-di-*tert*-butyl-4-hydroxytoluene (BHT) and potassium carbonate as base and thus the symmetrical unit **8** equipped with two different leaving groups was obtained as a colorless oil in a yield of 67% (Scheme 2).

Reaction of the two cyclophane units **5** and **8** by nucleophilic substitution afforded dimer **9** in a moderate yield of 48% (Scheme 3). Because both alkyl spacers were previously coupled to only one part of the cyclophane, homodimerization was excluded. By carefully adjusting the reaction conditions (Cs_2CO_3, acetone, 40°C, 16 h) only the iodide, as the better leaving group in nucleophilic substitution reactions, reacted. Before performing the intramolecular macrocyclization the protecting group was removed by photolytic debenzylation. Therefore the nitrobenzyl-protected alcohol **9** was irradiated for 5 h at room temperature with alternating 300 and 366 nm UV lamps in a Rayonet photochemical reactor (Scheme 3). To suppress the enrichment of various decomposition products of 2-nitrosobenzaldehyde, which is formed by photolytic cleavage of 2-nitrobenzyl groups, radical inhibitor BHT was added to the reaction mixture as reported by Mattei and Diederich.[39] After flash column chromatography (SiO_2; CH_2Cl_2/MeOH, 20:1), alcohol **10** was isolated in a yield of 97% (Scheme 3). The chloroalkylated phenol **10** underwent intramolecular macrocyclization to afford cyclophane **11** in an excellent yield of 72% (Scheme 3). To prevent oligomerization, the concentration of **10** in solution was kept low by adding the starting material slowly (30 h) to a suspension of cesium carbonate in acetonitrile at reflux.[39]

Even though the synthesis of cyclophane **11** was successfully accomplished, the initial goal of this synthesis was the development of a protocol for synthesizing large quantities in an easy and modular synthesis. Furthermore, the troublesome coupling of the two subunits **5** and **8** led to an overall moderate yield of 34% for the cyclization procedure, which

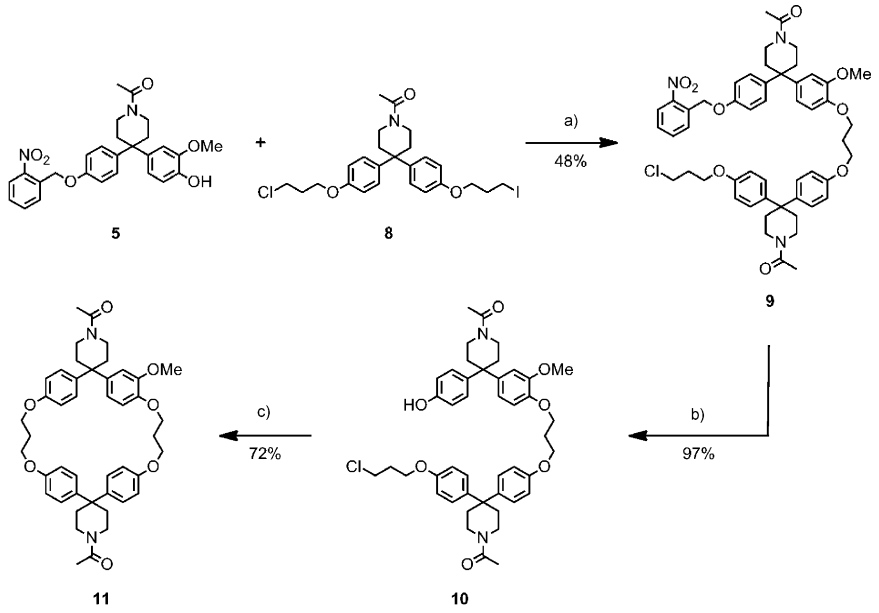

Scheme 3. Stepwise cyclization procedure towards monofunctionalized cyclophane **11**. Reagents and conditions: a) Cs_2CO_3, acetone, 40 °C, 16 h; b) BHT, THF, *hν*, RT, 5 h; c) Cs_2CO_3, MeCN, reflux, 36 h.

is in the range reported for intermolecular macrocyclizations but far from an optimal procedure.[38] Therefore it was decided to shorten the synthetic route mainly by using an intermolecular cyclization procedure.

Thus, to introduce one of the alkyl linkers, phenol **3** was substituted with 1,3-dibromopropane to give **12** in a yield of 71%. Addition of guaiacol to the alkene moiety of **12** led to **13** in a yield of 94% after column chromatography. Final nucleophilic substitution of the remaining phenol with 1,3-dibromopropane gave the desired monofunctionalized component **14** of cyclophane **11** in a yield of 91% as a colorless oil (Scheme 4).

For the intermolecular cyclization it turned out to be crucial to have two leaving groups with the same reactivity to avoid oligomerization. The monofunctionalized unit **14** was coupled to bis(hydroxyphenyl)-piperidine **15** by nucleophilic substitution under high dilution reaction conditions, which was synthesized following a literature protocol in a single step from *N*-acetylpiperidin-4-one and phenol in acidic media.[36] Cyclophane **11** was thus obtained as a white powder in a yield of 31% after column chromatography and precipitation with ethanol (Scheme 5), which is comparable to the overall yield of the stepwise cyclization procedure. Analyses of the side-products by ESI-MS documented the formation of trace amounts of the tetrameric product as well as the formation of higher oligomers. Furthermore, results of the analysis suggest that over a long reaction time (24 h) the amide was cleaved to a certain extent. Nevertheless, the simple purification procedure and the possibility of synthesizing the cyclophane precursors **14** and **15** in bulk made this strategy towards monofunctionalized cyclophane **11** the method of choice.

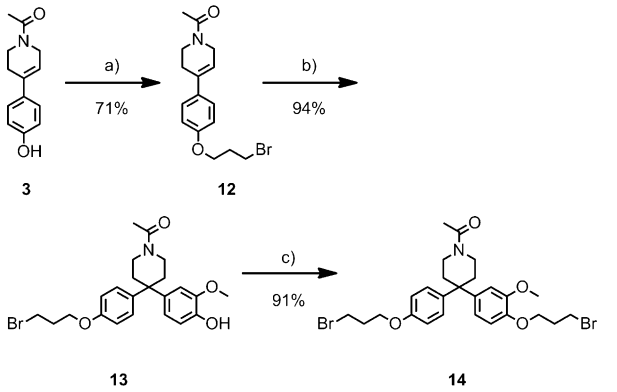

Scheme 4. Synthesis of the monofunctionalized cyclophane component **14**. Reagents and conditions: a) 1,3-dibromopropane, K_2CO_3, MeCN, reflux, 5 h; b) guaiacol, $BF_3{\cdot}OEt_2$, CH_2Cl_2, RT, 9 d; c) 1,3-dibromopropane, K_2CO_3, acetone, reflux, 20 h.

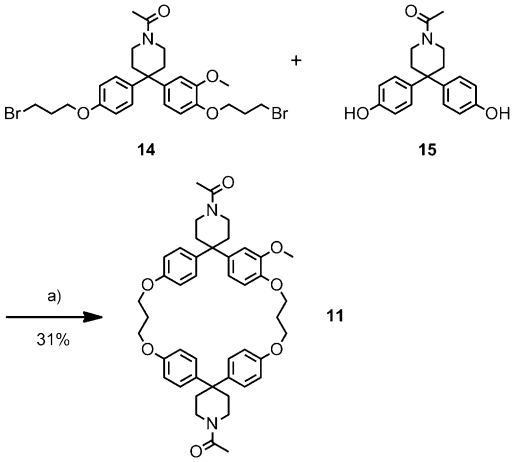

Scheme 5. Assembly of cyclophane **11** by an intermolecular approach. Reagents and conditions: a) Cs_2CO_3, acetonitrile, reflux, 20 h.

Having the desired monofunctionalized cyclophane **11** in hand, it was of interest to transform the masked functionality into a suitable reaction center for Sonogashira cross-coupling reactions. Therefore the methoxy group had to be cleaved without cleavage of the cyclophane alkoxy groups. The use of nucleophilic demethylation conditions turned out to be the method of choice. Therefore the cyclophane was treated with sodium thiomethoxide in dry DMF at 160 °C for 6 h.[43] After quenching with a 0.1 M aqueous HCl solu-

tion and recrystallization from methanol, the desired phenol **16**, which is insoluble in most common solvents, was obtained in an excellent yield of 98% (Scheme 6). Because

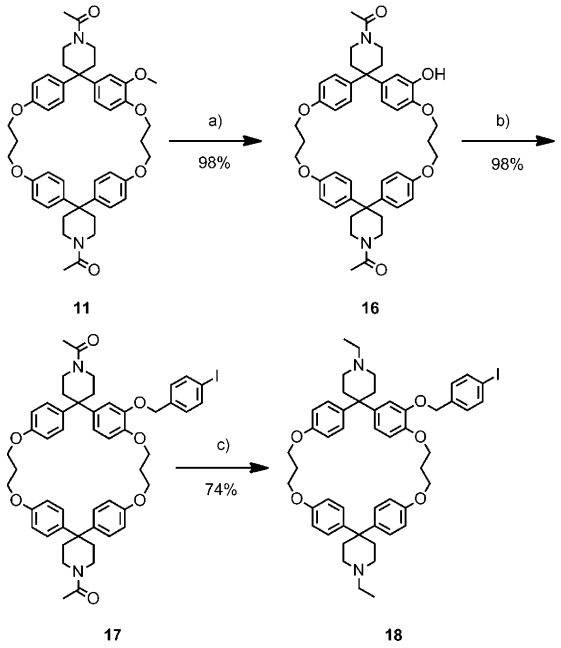

Scheme 6. Introduction of a benzyl linker bearing a suitable halide for Sonogashira cross-coupling reactions and activation of the piperidine nitrogen atom for subsequent alkylation. Reagents and conditions: a) sodium thiomethoxide, DMF, 160°C, 6 h; b) 4-iodobenzyl bromide, Cs_2CO_3, DMF, 85°C, 20 h; c) DIBAL-H, CH_2Cl_2, 0°C then RT, 4 h.

rather harsh reaction conditions had to be used to ensure full conversion, in some cases, nucleophilic aromatic substitution of thiomethoxide at one of the phenylene groups was observed. Demethylation with thiophenol or boron tribromide led to no conversion, as indicated by TLC. In the next step it was decided to introduce a 4-iodobenzyl group mainly to assist supramolecular aggregation by increasing the flexibility; directly linking the molecular rod to the cyclophane, which would require transformation of the free phenol **16** into a triflate, would potentially prevent the aggregation because of the resulting stiffness. The benzyl linker was installed by S_N2 reaction of 4-iodobenzyl bromide with phenol in the presence of cesium carbonate in DMF at 85°C. By using these reaction conditions, compound **17** was isolated after column chromatography in a yield of 98% (Scheme 6). The use of a weaker base like potassium carbonate did not lead to full conversion after 48 h. Before cross-coupling with the oligophenylene-ethynylene **22**, the acetyl protecting groups of the piperidinyl moiety were reduced to the corresponding alkyls to avoid the formation of possible byproducts. The reduction was performed by slowly adding DIBAL-H to a dilute solution of diamide **17** in dichloromethane at 0°C. After addition of the reducing agent, the reaction was allowed to warm to room temperature. This reaction turned out to be one of the crucial steps in the synthesis of monomer **1** because at room temperature not only the amides were reduced but also the iodobenzyl ether was cleaved to a certain extent (around 50%). Unfortunately, however, the reaction did not show full conversion at 0°C and small amounts of inseparable mono-reduced byproduct were observed by ESI-MS. Therefore the chosen reaction conditions are a compromise, and amine **18** was obtained in a yield of 74% (Scheme 6). The use of other reducing reagents like BH_3·THF led to partial defunctionalization of the iodide functionality and were therefore neglected.

The molecular wire **22** was synthesized starting from 1,4-diiodobenzene. In the first step, acetylenes with orthogonal protecting groups, namely trimethylsilylacetylene and dimethylpropargyl alcohol (HOP) were statistically cross-coupled. Product **19**, obtained in a yield of 45%, was then selectively deprotected on the HOP side with sodium hydroxide in toluene at reflux (Scheme 7).[44] The free acetylene **20** was

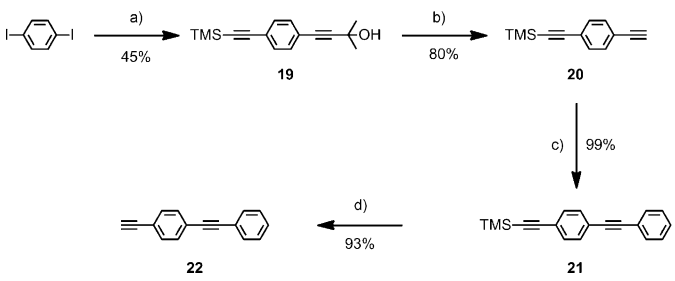

Scheme 7. Synthesis of the oligophenylene-ethynylene building block **22**. Reagents and conditions: a) $[PdCl_2(PPh_3)_2]$, CuI, DIPA, THF, RT, 1) TMS-acetylene, 4 h, 2) 2-methyl-3-butyn-2-ol, RT, 16 h; b) NaOH, toluene, 80°C, 1 h; c) 4-iodobenzene, $[PdCl_2(PPh_3)_2]$, CuI, DIPA, THF, RT, 4 h; d) TBAF, Ac_2O, AcOH, THF, 0°C then RT, 2 h.

then cross-coupled by means of a Sonogashira protocol with iodobenzene (Scheme 7). In the final step, the TMS protecting group was removed by tetrabutylammonium fluoride (TBAF) to yield the desired OPE **22** in a total yield of 33% over four steps, including one statistical Sonogashira cross-coupling reaction.

The OPE rod **22** was then cross-coupled with the cyclophane by using $[Pd(dba)_2]$, triphenylphosphine, CuI, and diisopropylamine (DIPA) in THF at room temperature. In the presence of catalysts such as $[Pd(PPh_3)_4]$ or $[PdCl_2(PPh_3)_2]$ or without a large excess of base, no conversion was observed. The crude was purified by extraction and column chromatography to yield the desired scaffold **23** in a yield of 92% as a white solid (Scheme 8). The tertiary amines were finally alkylated in dichloromethane by using freshly distilled iodoethane. After stirring for 5 days at room temperature, monomer **1** was isolated by column chromatography on silica that had been preconditioned with a 12% (w/v) methanolic solution of sodium bromide,[45] eluting with a mixture of dichloromethane and 5% methanol. Ion-exchange chromatography (DOWEX 1X8, 200–400 mesh, Cl^-) gave the desired product **1** comprising a hydrophobic molecular rod and a terminal hydrophilic loop as the chloride salt

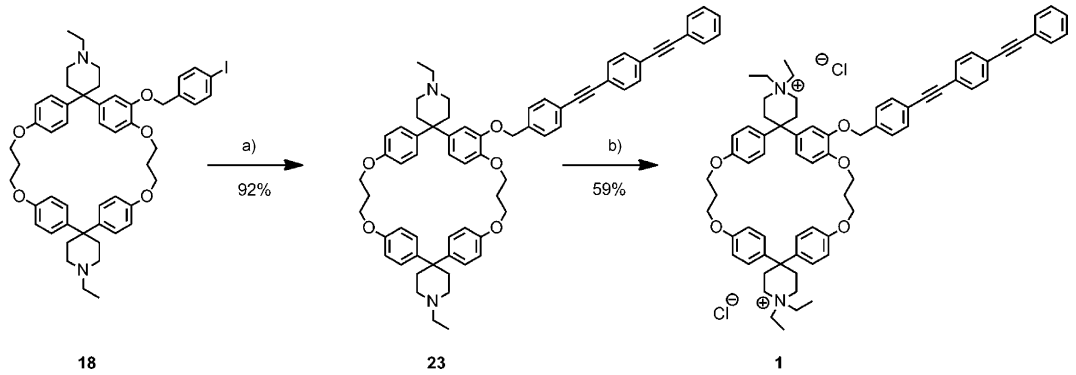

Scheme 8. Final assembly of the amphiphilic monomer **1**. Reagents and conditions: a) OPE **22**, $[Pd(dba)_2]$, PPh_3, CuI, DIPA, THF, RT, 3 h; b) iodoethane, CH_2Cl_2, RT, 5 d, then ion exchange (DOWEX 1X8, 200–400 mesh Cl^-).

in a yield of 59% as an off-white hygroscopic solid (Scheme 8).

According to the procedure described herein, product **1**, comprising a hydrophobic oligophenylene-ethynylene rod and a terminal hydrophilic loop, was synthesized in 21 steps by an intramolecular stepwise cyclophane assembly or in 17 steps by intermolecular macrocyclization. It has been shown that cyclophane **11** can be synthesized in large quantities (2 g) and interlinking of the hydrophobic and hydrophilic components **18** and **22** is possible in good yields. The hermaphroditic monomer **1** was characterized by low-resolution ESI-MS and ^{1}H NMR spectroscopy (see the Supporting Information).

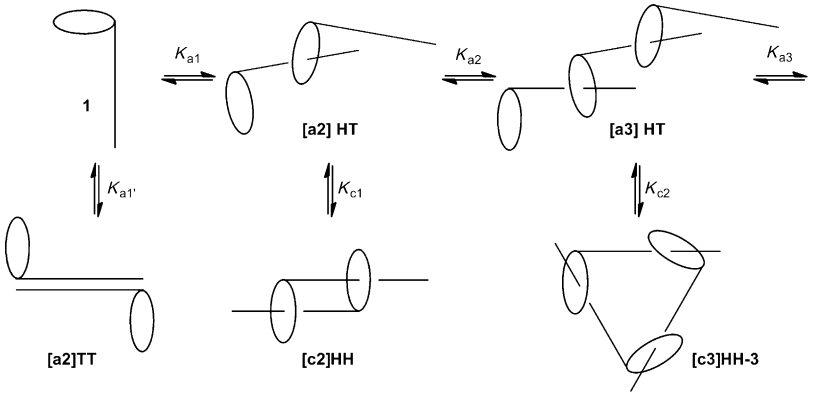

Figure 2. Possible aggregates formed by amphiphile **1** in polar solvents.[26,28]

NMR aggregation studies: With the desired hermaphroditic monomer **1** in hand it was of interest to study its aggregation behavior in polar solvents by NMR spectroscopy. To make use of the strong nonclassical hydrophobic effect, the aggregation studies were solely focused on the chloride salt of monomer **1**, for which the best water-solubility was expected, as reported by Diederich et al.[36] As outlined in the introduction, such amphiphilic molecules can potentially form various aggregates (Figure 2).[28] Monomer **1** may, as shown in Figure 2, form three different dimer structures excluding aggregation of the organic ions as well as assemblies in which the OPE rod comes into close proximity with the spiro-piperidinyl moieties. The formation of [c2]daisy chains (**[c2]HH**) is well known in the literature and these conformations are often thermodynamically stable aggregates that prevent the formation of longer oligomers.[27] Also, the aggregation of two hydrophobic OPE rods (**[a2]TT**) is possible, but it is expected that such a binding is weaker than the inclusion of the rod in host cavities and therefore causes, because of the reversible aggregation, no interruption of oligomerization.

The formation of an acyclic head-to-tail dimer (**[a2]HT**) can be seen as the first propagation step towards polymerization. Nevertheless, each possible *n*-mer of the propagating chain has the possibility of forming, because of the expected reversible binding, the cyclic version of the oligomer. The hypothetical formation of this variety of aggregates makes a detailed analysis difficult. ^{1}H NMR titrations, DOSY NMR spectroscopy, HRMS, and fluorescence measurements were performed for this purpose.

Previous publications have shown that concentration-dependent ^{1}H NMR spectroscopy can be used to determine the aggregation number n and the association constant K_a.[34,46,47] Thus, ^{1}H NMR spectra were recorded at constant temperature at different concentrations of monomer **1** in a 3:2 mixture of D_2O/[D_4]methanol (Figure 3).

The NMR spectra show that the protons are under fast exchange on the NMR timescale. Therefore the observed chemical shifts (δ_{obs}) can be expressed as the sum of the chemical shifts of the monomer (δ_{mon}) and of the individual aggregates (δ_{agg}), each one as a weighted average of its molar fraction [Equation (1)].[48]

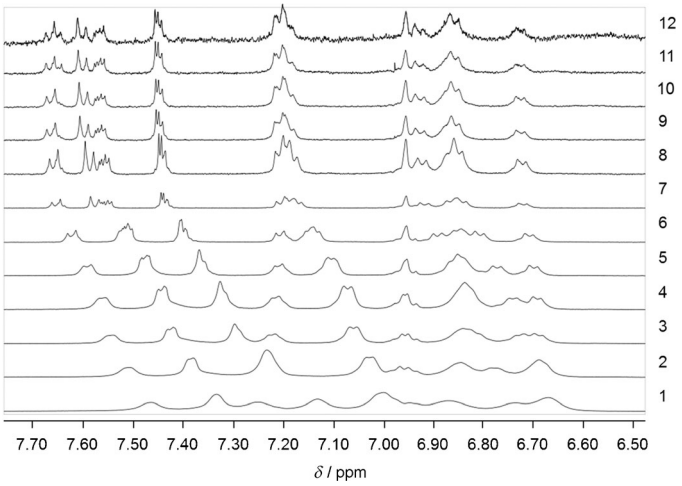

Figure 3. Stacked ^{1}H NMR spectra recorded with a 500 MHz spectrometer showing the aromatic region of monomer **1**. 1) 7.96, 2) 3.98, 3) 2.99, 4) 1.99, 5) 1.49, 6) 1.12, 7) 0.32, 8) 0.22, 9) 0.091, 10) 0.055, 11) 0.026, 12) 0.014 mM.

$$\delta_{obs} = \delta_{mon}(C_{mon}/C_{tot}) + \delta_{agg1}(C_{agg1}/C_{tot}) + \delta_{agg2}(C_{agg2}/C_{tot}) + \text{etc} \quad (1)$$

When assuming that the concentration (C) of an aggregate that is predominant in a certain concentration range remains constant above a certain concentration, a plot of δ_{obs} versus the inverse concentration ($1/C$) should give a straight line after each individual change in aggregation. The intersection of these lines then gives directly the critical aggregation concentration (CAC) for each individual aggregate.[46] For simplification, only one equilibrium was considered for each aggregate and concentration range, and cooperative effects were excluded, which means that for all equilibria the same association constant was assumed ($K_{a1}=K_{a2}=K_{a3}$ etc.). Thus, Equation (1) simplifies to a linear function. A representative plot of δ_{obs} for one proton of the amphiphile **1** (assigned to the OPE unit by 2D NMR spectra) against the inverse total concentration ($1/C_{tot}$) is illustrated in Figure 4, which indicates two critical aggregation concentrations at 0.941 ($1/C_{tot}=1062.7\,M^{-1}$) and 3.03 mM ($1/C_{tot}=330.0\,M^{-1}$). Below 1 mM, the observed chemical shift remains constant, which indicates that only one aggregate or monomer is dominant. No further conclusions can be drawn above 3 mM because the ^{1}H NMR signals broaden and therefore further assignment of individual protons is impossible (Figure 3).

Large upfield shifts of the aromatic signals assigned to the OPE unit were observed above the CAC of 1 mM in contrast to the proton chemical shifts below 7.00 ppm for which only weak shifts were observed (Figure 3). By threading the OPE rod into the cavity of the cyclophane, the phenyl protons of the rod experience a ring current from the electron-rich aromatic systems in the cavity wall, which leads to an induced chemical-shift change. Thus, the large upfield shift can be seen as the first evidence for threading of the OPE rod into the cavity of the cyclophane.

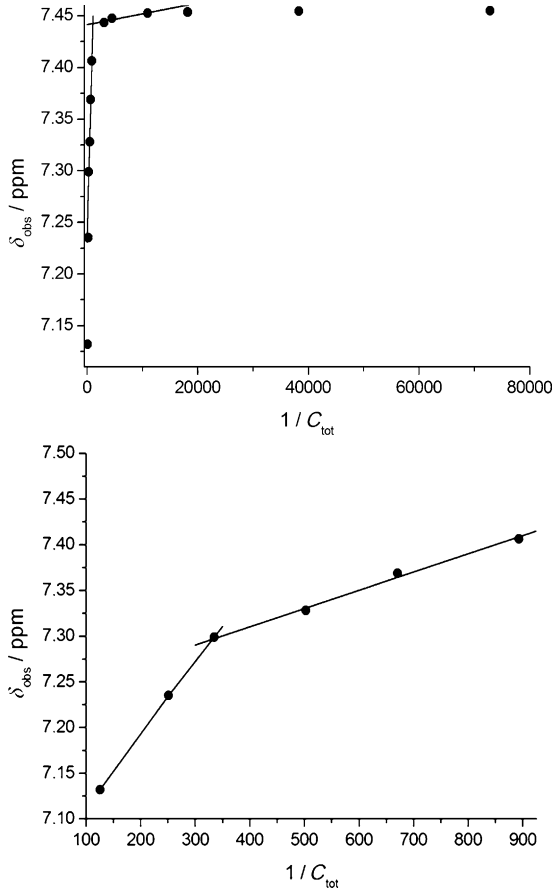

Figure 4. Top: Plot of the observed chemical shift (δ_{obs}) against the inverse of the concentration ($1/C$) of monomer **1**. Straight lines represent linear regression analyses; from the intersection, the critical aggregation concentration (CAC) was calculated. Bottom: The second CAC at higher concentrations.

As mentioned above, the ^{1}H NMR data can also be employed to obtain the aggregation number n and the association constant K_a from Equation (2), which describes an equilibrium in which n monomers form a single aggregate.[34,46–48]

$$\ln[C_{tot}(|\delta_{obs}-\delta_{mon}|)] = n\ln[C_{tot}(|\delta_{agg}-\delta_{obs}|)] + \ln K_a + \ln n - (n-1)\ln(|\delta_{agg}-\delta_{mon}|) \quad (2)$$

Plots of $\ln[C_{tot}(|\delta_{obs}-\delta_{mon}|)]$ versus $\ln[C_{tot}(|\delta_{agg}-\delta_{obs}|)]$ (Figure 5) give a straight line from which the slope and the intercept can be calculated to yield n and K_a, respectively. By plotting δ_{obs} against the total concentration and extrapolating to zero amphiphile, the chemical shift of the monomer (δ_{mon}) can be approximated.[47] Extrapolation of the concentration to infinity yielded the chemical shift of the aggregate (δ_{agg}; see the Supporting Information).[47]

The variation of the slopes in Figure 5 clearly demonstrate that the data obtained by NMR titration can be divided into three different concentration ranges, as has already been shown by the plot of the observed chemical shifts against the inverse concentration (Figure 4). An aggregation

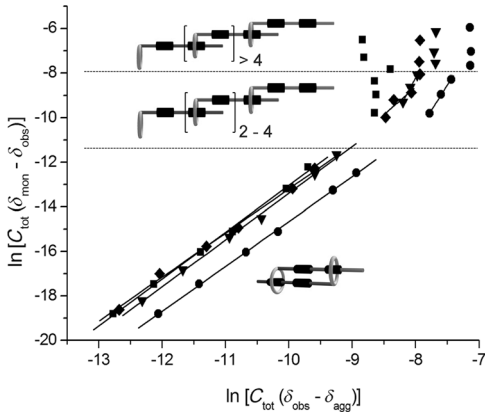

Figure 5. Plot of $\ln[C_{tot}(|\delta_{obs}-\delta_{mon}|)]$ against $\ln[C_{tot}(|\delta_{agg}-\delta_{obs}|)]$. Straight lines represent linear regression analyses from which the aggregation number n and K_a were calculated.

number of $n=2$ was obtained by analysis of the concentration range between 0.014–1 mM. Different aromatic signals as well as the shifting signals in the aliphatic region lead to relative narrow aggregation values between 1.97–2.10, which strongly suggests the formation of dimeric structures. Furthermore, by analysis of just the concentration range in which dimer formation is observed, an association constant of $K_a=9.8\times10^6\,M^{-1}$ was obtained when the chemical shift of the aggregate was replaced by the shift of the dimer. Interpretation of the association constant has to be taken with caution because it was assumed that in each concentration range only one aggregate is dominant. The concentration range in which the transition from monomer to dimer can be observed was unfortunately not reached in this NMR titration due to instrumentation limits. By closer inspection of the titration curve obtained by plotting δ_{obs} against the concentration, it became clear that only the first part of the expected dimer plateau was reached, which makes a precise prediction of the monomer chemical shift (δ_{mon}) impossible.

In the concentration range between the two CACs, aggregation numbers of between 4.5 and 6 were obtained. Above 3 mM, a precise estimation of the aggregation number was not possible due to the strong broadening of the proton peaks, but data suggest $n>6$ (or even $n>10$). Even though the protons are in fast exchange on the NMR timescale, the wide concentration range in which dimerization can be observed provides evidence for a strong hydrophobic effect. It is, however, safe to conclude that higher oligomers at concentrations above 1 mM are formed, as indicated by the plots in Figure 5. Furthermore, the strong broadening of the proton signals, which is typical of polymer formation due to increased viscosity, strongly supports this finding. DOSY measurements were performed on amphiphile **1** and a non-self-aggregating compound as reference to determine the size of the main aggregate in polar solvent at a concentration at which NMR titration studies indicate mainly dimer existence (200 μM). Therefore the hydrodynamic radii of the aggregates as well as their relative volumes compared with monomer **1** were calculated (see the Supporting Information). According to the calculations, the measured substances are 1.48 times larger than the monomer, which strongly supports the self-aggregation observed previously in the NMR titration experiments. The fact that this value is less than 2, which is the value expected for acyclic dimers, strongly indicates the formation of [c2]daisy chains. Thus, it has been shown that the dimer is the predominant species over a broad concentration range, which allows scope for functionalization to enable subsequent polymerization.

Fluorescence aggregation studies: To gain further insight into the dimerization of the hermaphroditic compound **1**, a fluorescence titration in the concentration range of 0.028 to 6.6×10^{-6} mM was performed. Compound **1** in a mixture of H_2O/methanol (3:2) was excited at the absorption wavelength of the π–π* transition of the hydrophobic oligophenylene–ethynylene moiety (321 nm). Emission at 355 and 369 nm with a shoulder at around 380 nm was observed, which decreases with decreasing concentration, as illustrated in Figure 6.

Comparison of the emission spectra of amphiphile **1** in water/methanol (3:2) and dichloromethane, in which only the monomer should be present, clearly demonstrates that the intensity of emission of **1** in polar solvent is lower at the same concentration (see the Supporting Information). Even though a decrease in intensity is expected due to solvent ef-

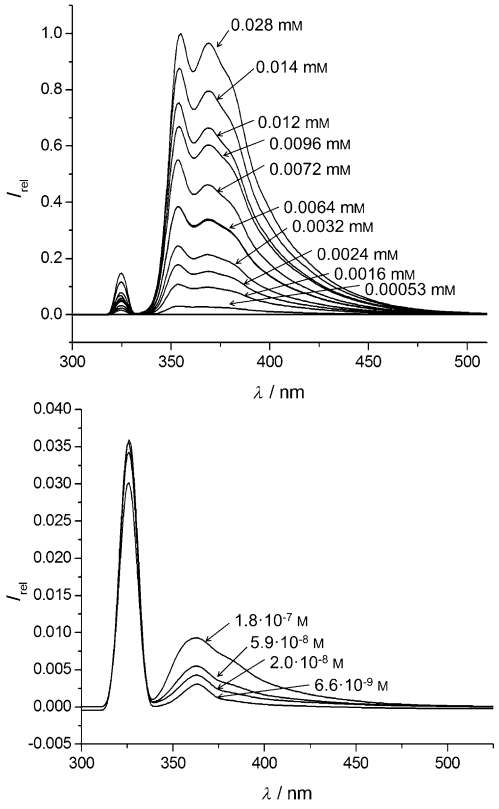

Figure 6. Top: Emission spectra of compound **1** in H_2O/methanol (3:2) in a concentration range of 0.028 to 6.6×10^{-6} mM. Bottom: The emission of **1** at the lowest concentrations.

fects, the dramatic decrease is indicative of the inclusion of the OPE rod in the cavity and is a result of the insulating nature of the macrocycles. Furthermore, because the emission spectra of the monomer and dimer show the same bands, excimer formation can be excluded. Hence, possible dimeric structures in which the hydrophobic rods aggregate outside the cavity (**[a2]TT**) is unlikely.[34] Because it is expected that a dimer such as the [c2]daisy chain should allow for excimer formation, this finding suggests an unfavorable arrangement of the two hydrophobic rods with respect to each other in the cavity or a structure in which only one rod is embedded in the cavity of another, as in the [a2]daisy chain.

A plot of the inner filter effect corrected relative intensities against concentration shows dimer formation down to a CAC of 1.83×10^{-6} M. Below this CAC, the intensities decrease linearly with a decreased slope (Figure 7).

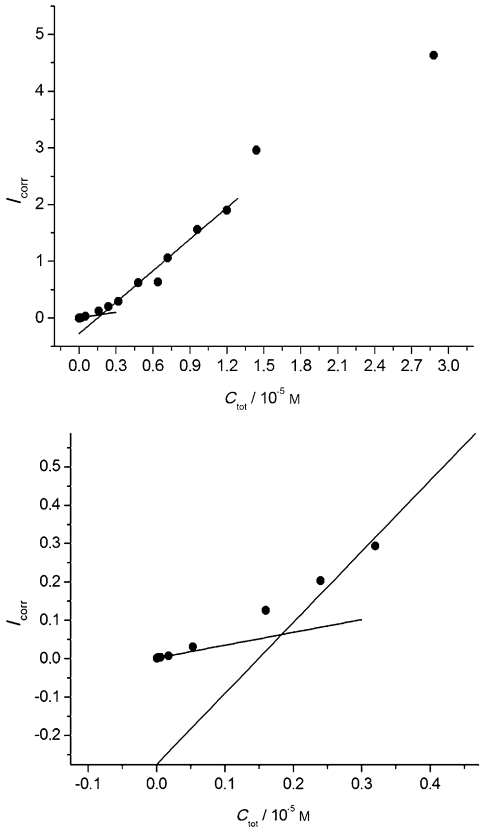

Figure 7. Top: Plot of the relative intensities (I_{corr}) at 355 nm against the concentration (C_{tot}). Bottom: Graphical extrapolation to estimate the CAC is shown.

The NMR titrations demonstrated that at the concentrations used to record the fluorescence spectra, dimerization is the dominant process. The association constant K_a can thus be expressed by Equation (3).

$$K_a = C_{dim}/C_{mon}^2 \quad (3)$$

The total amphiphile concentration is therefore given by Equation (4).

$$C_{tot} = C_{mon} + 2C_{dim} \quad (4)$$

Substitution for the dimer concentration gives Equation (5).

$$C_{tot} = C_{mon} + 2K_aC_{mon}^2 \quad (5)$$

Because it has been shown that the fluorescence of the monomer is significantly higher than that of the dimer, a good approximation to estimate K_a is to assume that the fluorescence of the monomer is directly proportional to its concentration. Hence, Equation (5) can be written as demonstrated by Margalit et al.[49,50] as Equation (6) in which k is an experimental coefficient. From the slope and the intercept of a plot of C_{tot}/I_{corr} against I_{corr}, the association constant was calculated to be 1.33×10^{6} M^{-1} (Figure 8).

$$C_{tot}/I_{corr} = k + 2k^2K_aI_{corr} \quad (6)$$

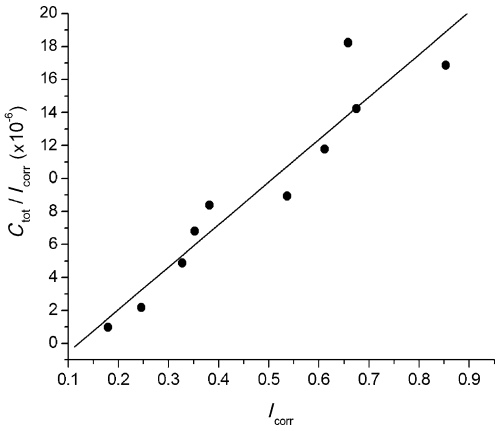

Figure 8. Plot of C_{tot}/I_{corr} against I_{corr} for estimation of the association constant K_a.

The rather high association constant is in good agreement with the observation of a strong hydrophobic effect as well as with the association constants reported by Anderson et al. for the threading of Diederich-type cyclophanes with dicationic oligophenylene-ethynylenes.[51] Despite the fact that direct evidence for the formation of daisy-chain aggregates in solution was not obtained, mainly due to the complicated ^{1}H NMR spectra, the high association constant, the significant upfield shifts of aromatic signals with increasing concentration, the observation of dimers over a broad concentration range and at very low concentrations, and the strongly reduced emission in water/methanol mixtures are strong indicators that it was possible to design and synthesize an amphiphilic monomer that can form daisy chains. Furthermore, it has been shown that the nature of these daisy chains can be varied just by changing the concentration. Attempts to grow single crystals suitable for X-ray

analysis to gain direct proof for aggregation were unfortunately not successful with the chloride salt of monomer **1**.

High-resolution ESI-MS aggregation studies: Direct proof for the formation and stability of aggregates in the gas phase was obtained by HRMS (Figure 9). Analysis of a

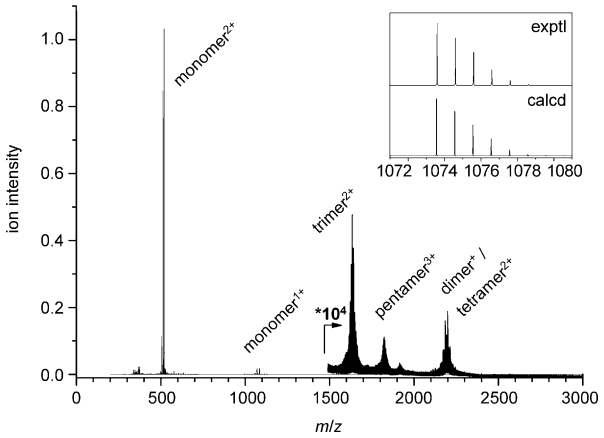

Figure 9. High-resolution ESI-MS spectrum of compound **1** showing the formation of dimers to pentamers. Inset: Comparison of the measured and calculated isotope patterns for $[M\mathrm{Cl}]^+$.

10^{-5} M solution of **1** in H_2O/methanol (3:2) by employing a nanospray source revealed oligomers of general composition $M_xCl_y^{z+}$, in which M is the dicationic form of the monomer. Accordingly, these oligomers carry a positive charge of $z = 2x-y$. Mass/charge ratios corresponding to dimers, trimers, tetramers, and pentamers were observed at this rather low concentration. Note that due to ion exchange of the chloride anions with other ions in aqueous solution, peak broadening was observed for the oligomers.

The peak with the highest intensity in this mass spectrum is the monomer peak, which is not surprising because the ions become isolated from the solvent in the spray process thereby reducing the driving force for aggregation. Despite the fact that the aggregation behavior of hermaphroditic daisy-chain monomer **1** in solution and in the gas phase cannot be directly compared, especially because of the missing hydrophobic effect on the one hand and the prevailing electrostatic interaction on the other, the observation of oligomers in the gas phase together with the results of ^{1}H NMR and emission spectroscopic analyses in solution, demonstrates the high potential of this new binding concept for the formation of long oligomeric daisy chains.

Conclusion

Daisy-chain monomer **1** comprising an OPE and a cyclophane loop has successfully been synthesized in excellent yields, and cyclophane **11** can be synthesized on a large scale. Owing to the inspirational work of Diederich and coworkers, it was possible to synthesize monofunctionalized cyclophane **11** by two different pathways and the hydrophobic OPE **22** was synthesized by classical Sonogashira cross-coupling reactions. NMR titration experiments showed the formation of dimers up to a concentration of 1 mM. Above this concentration, evidence for aggregation to form larger oligomers was found by graphic determination of the aggregation number. Fluorescence studies indicate that dimerization occurs at concentrations as low as 10^{-7} M. The reduced fluorescence intensity observed for the amphiphile **1** in the protic solvent mixture methanol/water compared with in dichloromethane suggests the inclusion of two rods in cavities forming a thermodynamically stable [c2]daisy chain, which is further supported by a high association constant K_a. It has been demonstrated that such aggregation behavior as a result of hydrophobic effects can play a major role in the controlled assembly of mechanically interlinked polymers. It is now of interest to study the effect of functionalization of the hydrophobic rod on the generation of well-defined mechanically interlinked macromolecules. The influence of counterions on the aggregation behavior is currently under investigation.

Experimental Section

General remarks: All chemicals were directly used in the syntheses without purification unless otherwise noted. Dry solvents were purchased from Fluka. Solvents for chromatography and extractions were distilled before use. When the Schlenk technique was used, the solvents were degassed with argon for several minutes. Silica gel 60 (40–63 μm) from Fluka or SilicaFlash P60 (40–63 μm) from Silicycle were used for column chromatography. TLC was performed on silica gel 60 F_{254} glass plates with a thickness of 0.25 mm from Merck. Characterizations were performed with the following instruments: ^{1}H and ^{13}C NMR spectra were recorded with a Bruker DPX-NMR (400 MHz) or DRX-500 (500 MHz) spectrometer; the *J* values are given in Hz. Solvents were obtained from Cambridge Isotope Laboratories. All spectra were recorded at 298 K. Mass spectra were recorded with a Finnigan MAT 95Q spectrometer (EI) and an Bruker esquire 3000 plus spectrometer (ESI). Elemental analyses were carried out on a varioMICROcube from elementar. HRMS were recorded by the group of Schürch at the university of Bern on a LTQ Orbitrap XL from Thermo Fisher Scientific using a nanoelectrospray ion source, except for monomer **1**, which was measured at the Karlsruhe Institute of Technology (see below for details).

NMR titrations: A stock solution of monomer **1** (8.84 mg) in D_2O/[D_4]methanol (3:2, 0.8 mL) was prepared. Other concentrations of monomer **1** were obtained by dilution of this solution. NMR spectra of the corresponding samples were recorded with a Bruker DRX-500 (500 MHz) spectrometer at 295 K. Solvents were obtained from Cambridge Isotope Laboratories. The samples were locked on [D_4]methanol. To assign the peaks in the individual spectra, COESY spectra were recorded for each individual sample.

NMR diffusion experiments: Self-diffusion measurements were performed on samples of amphiphile **1** and a reference compound lacking the OPE moiety with the bipolar gradient pulse sequence of Wu et al.[52] by using a Bruker Avance III NMR spectrometer operating at 600.13 MHz. The instrument was equipped with a 5 mm BBFO smart probe with a shielded z-gradient coil and a GAB gradient amplifier (10 A, maximum gradient strength 52.5 G cm^{-1}).

All samples were dissolved in a mixture of D_2O and [D_4]methanol (3/2, v/v). The diffusion experiments were performed at 298 K and the temperature was calibrated by using a methanol standard to an accuracy of ±0.2 K. The gradient strength was calibrated by using a Shigemi tube

filled with H_2O to a height of 4.0 mm and imaging this water cylinder.[53] The resulting gradient calibration was validated by determining the diffusion coefficient of water at 298 K, which reproduced the literature value within 5%.

Twelve single diffusion experiments with constant diffusion times (40 ms) and gradient lengths (2.5 ms) were performed, and the gradient strength was varied between 5 and 95% of the maximum strength. The decrease in the intensity of the signal of interest was determined and fitted with the Bruker *t*1/*t*2 software package suitable for DOSY experiments, which is included in the instrument software.[54]

Fluorescence measurements: A stock solution of monomer **1** (0.48 mg) in MilliQ water/methanol (3:2, 3 mL) was prepared. Other concentrations were obtained by dilution of this solution. Emission spectra were recorded with a Shimadzu RF-5301 PC spectrofluorophotometer using 1 cm 115F-QS Hellma cuvettes at room temperature in the presence of air. The excitation wavelength was 321 nm, which was determined by UV/Vis spectroscopy. The following instrument parameters were used: Excitation slit width 1.5 nm, emission slit width 3 nm, response time 2.0 s, and sampling interval 1.0 nm.

ESI mass spectrometry: Mass spectrometric characterization was performed on a hybrid quadrupole/ion mobility/time-of-flight mass spectrometer (SYNAPT G2-S HDMS, Waters Inc. Milford, MA, USA). The instrument was equipped with a nanospray source with gold-coated tips and a spray voltage of 1200 V. Solutions of monomer **1** in MilliQ water/methanol (3/2, v/v) at a concentration of $\sim 10^{-5}$ M were freshly prepared before spraying. The time-of-flight mass spectra were analyzed by using Waters' MassLynx 4.1 software package.

Synthesis of 1,1″-diactyl-5′-methoxydispiro[piperidine-4,2′-(7,11,21,25-tetraoxacyclopenta[24.2.2.2^{3,6}.2^{12,15}.2^{17,20}]hexatriaconta-3,5,12,14,17,19,26,28,29,31,33,35-dodecaene)-16,4″-piperidine] (11) by the intermolecular route: Cesium carbonate (5.64 g, 10.0 equiv, 17.1 mmol), bis-phenol **15** (534 mg, 1.00 equiv, 1.72 mmol), and dialkyl dibromide **14** (1.00 g, 1.00 equiv, 1.72 mmol) were suspended in acetonitrile (0.6 L) and heated at reflux for 20 h. After cooling to room temperature, the precipitate was filtered off and the filtrate was concentrated. The residue was taken up in dichloromethane and the insoluble white solid was again filtered off. The filtrate was again concentrated and the remaining crude purified by column chromatography (SiO_2; dichloromethane, 5% MeOH). The white solid product was precipitated with EtOH, filtered, and washed with EtOH and a small amount of diethyl ether (31%).

R_f = 0.36 (CH_2Cl_2, 5% MeOH); m.p. 266 °C; ^{1}H NMR (400 MHz, $CDCl_3$, 25 °C, TMS): δ = 7.16–7.07 (m, 6H; Ar-H), 6.76–6.67 (m, 8H; Ar-H), 6.63–6.59 (m, 1H; Ar-H), 4.08–3.98 (m, 8H), 3.85–3.74 (m, 1H), 3.68–3.58 (m, 5H, including s at 3.62 (OCH_3)), 3.58–3.40 (m, 5H), 2.46–2.27 (m, 8H), 2.24–2.11 (m, 4H), 2.07 ppm (s, 6H; 2×(CO)CH_3); ^{13}C NMR (101 MHz, $CDCl_3$, 25 °C, TMS): δ = 168.9 (C_q, 2C; C=O), 157.3 (C_q, 1C), 157.2 (C_q, 1C), 157.2 (C_q, 1C), 149.4 (C_q, 1C), 147.0 (C_q, 1C), 140.0 (C_q, 1C), 138.9 (C_q, 1C), 138.6 (C_q, 1C), 138.0 (C_q, 1C), 127.2 (C_t, 2C), 126.9 (C_t, 4C), 118.0 (C_t, 1C), 114.8 (C_t, 2C), 114.8 (C_t, 2C), 114.7 (C_t, 2C), 113.1 (C_t, 1C), 110.4 (C_t, 1C), 64.7 (C_s, 1C), 63.6 (C_s, 1C), 63.4 (C_s, 1C), 63.3 (C_s, 1C), 55.9 (C_p, 1C, OCH_3), 43.7 (C_q, 1C), 43.6 (C_s, 2C), 43.1 (C_q, 1C), 38.6 (C_s, 1C), 38.6 (C_s, 1C), 36.0 (C_s, 1C), 35.8 (C_s, 1C), 35.1 (C_s, 1C), 34.8 (C_s, 1C), 29.7 (C_s, 1C), 29.6 (C_s, 1C), 21.6 ppm (C_p, 2C, (CO)CH_3); MS (ESI, positive ion mode, MeCN): *m*/*z* (%): 771 [*M*+K]$^+$, 755 [*M*+Na]$^+$, 733 [*M*+H]$^+$; elemental analysis calcd (%) for $C_{45}H_{52}N_2O_7$: C 73.75, H 7.15, N 3.82; found: C 73.73, H 6.96, N 3.82.

1,1″-Diactyl-5′-hydroxydispiro[piperidine-4,2′-(7,11,21,25-tetraoxacyclopenta[24.2.2.2^{3,6}.2^{12,15}.2^{17,20}]hexatriaconta-3,5,12,14,17,19,26,28,29,31,33,35-dodecaene)-16,4″-piperidine] (16): Cyclophane **11** (664 mg, 1.00 equiv, 0.906 mmol) and sodium thiomethoxide (317 mg, 5.00 equiv, 4.53 mmol) were dissolved in DMF (70 mL) and heated at 160 °C under an argon atmosphere for 6 h. Then 0.1 M aq. HCl (46 mL) was added and the solvents removed under vacuum. The residue was taken up in water and the suspension was filtered. The remaining pale-beige solid was washed once with diethyl ether (10 mL). The white powder was recrystallized from methanol (98%).

R_f = 0.35 (CH_2Cl_2, 5% MeOH); m.p. 232 °C; ^{1}H NMR (400 MHz, $CDCl_3$, 25 °C, TMS): δ = 7.16–7.05 (m, 6H; Ar-H), 6.79–6.60 (m, 9H; Ar-H), 5.64 (br s, 1H; OH), 4.14–4.07 (m, 2H; phenol-O-CH_2), 4.06–3.98 (m, 6H; Ar-O-CH_2), 3.72–3.57 (m, 4H), 3.55–3.44 (m, 4H), 2.47–2.28 (m, 8H), 2.25–2.12 (m, 4H), 2.07(s, 3H; (CO)CH_3), 2.06 ppm (s, 3H; (CO)CH_3); ^{13}C NMR (101 MHz, $CDCl_3$, 25 °C, TMS): δ = 168.9 (C_q, 2C, C=O), 157.1 (C_q, 1C), 157.1 (C_q, 1C), 156.8 (C_q, 1C), 145.7 (C_q, 1C), 144.2 (C_q, 1C), 140.3 (C_q, 1C), 139.1 (C_q, 1C), 138.5 (C_q, 1C), 138.4 (C_q, 1C), 127.0 (C_t, 4C), 126.9 (C_t, 2C), 116.9 (C_t, 1C), 114.8 (C_t, 2C), 114.7 (C_t, 2C), 114.6 (C_t, 2C), 112.9 (C_t, 1C), 111.6 (C_t, 1C), 65.1 (C_s, 1C), 63.9 (C_s, 1C), 63.3 (C_s, 1C), 63.3 (C_s, 1C), 63.3 (C_s, 1C), 43.6 (C_s, 1C), 43.6 (C_s, 1C), 43.2 (C_q, 1C), 43.1 (C_q, 1C), 38.6 (C_s, 1C), 35.8 (C_s, 1C), 35.8 (C_s, 1C), 34.8 (C_s, 1C), 34.8 (C_s, 1C), 29.6 (C_s, 1C), 29.4 (C_s, 1C), 21.6 ppm (C_p, 2C; (CO)CH_3); MS (ESI, positive ion mode, MeCN): *m*/*z* (%): 757 [*M*+K]$^+$, 741 [*M*+Na]$^+$, 719 [*M*+H]$^+$; HRMS (ESI): *m*/*z* calcd for [$C_{44}H_{50}N_2O_7$+H]$^+$: 719.3691; found: 719.3691.

1,1″-Diactyl-5′-(4-iodobenzyloxy)dispiro[piperidine-4,2′-(7,11,21,25-tetraoxacyclopenta[24.2.2.2^{3,6}.2^{12,15}.2^{17,20}]hexatriaconta-3,5,12,14,17,19,26,28,29,31,33,35-dodecaene)-16,4″-piperidine] (17): Alcohol **16** (150 mg, 1.00 equiv, 0.209 mmol), 4-iodobenzyl bromide (98.0 mg, 1.50 equiv, 0.314 mmol), and cesium carbonate (138 mg, 2.00 equiv, 0.418 mmol) were suspended in dry DMF (12 mL) under an argon atmosphere. The reaction mixture was heated at 85 °C for 20 h. Afterwards, the solvent was evaporated and the residue taken up in dichloromethane and water. The layers were separated and the aqueous layer extracted three times with dichloromethane. The combined organic layers were washed with water and brine, dried with sodium sulfate, filtered, and concentrated. The crude was purified by column chromatography (SiO_2; dichloromethane then dichloromethane, 2.5% MeOH). The desired product **17** was obtained as a white powder (98%).

R_f = 0.39 (CH_2Cl_2, 5% MeOH); m.p. 137 °C; ^{1}H NMR (400 MHz, $CDCl_3$, 25 °C, TMS): δ = 7.64 (d, ^3J(H,H) = 8 Hz, 2H; iodobenzene-H2), 7.12–7.06 (m, 4H; Ar-H), 6.98 (d, ^3J(H,H) = 8 Hz, 2H; Ar-H), 6.94 (d, ^3J(H,H) = 8 Hz, 2H; Ar-H), 6.75–6.67 (m, 8H; Ar-H), 6.46 (d, ^4J(H,H) = 2 Hz, 1H; Ar-H), 4.73 (s, 2H; iodobenzene-CH_2O), 4.09–3.99 (m, 8H; Ar-OCH_2), 3.72–3.61 (m, 3H), 3.53–3.36 (m, 5H), 2.42–2.33 (m, 4H), 2.30–2.12 (m, 8H), 2.06 ppm (s, 6H; 2×(CO)CH_3); ^{13}C NMR (101 MHz, $CDCl_3$, 25 °C, TMS): δ = 168.4 (C_q, 2C; C=O), 157.1 (C_q, 1C), 157.1 (C_q, 1C), 157.0 (C_q, 1C), 147.7 (C_q, 1C), 147.5 (C_q, 1C), 139.8 (C_q, 1C), 138.7 (C_q, 1C), 138.6 (C_q, 1C), 137.7 (C_q, 1C), 137.5 (C_t, 2C), 137.3 (C_q, 1C), 129.4 (C_t, 2C), 126.9 (C_t, 2C), 126.8 (C_t, 4C), 118.7 (C_t, 1C), 114.7 (C_t, 4C), 114.6 (C_t, 2C), 114.3 (C_t, 1C), 113.7 (C_t, 1C), 93.0 (C_q, 1C; C-I), 70.4 (C_s, 1C; iodobenzene-CH_2O), 64.6 (C_s, 1C), 63.3 (C_s, 1C), 63.2 (C_s, 1C), 63.2 (C_s, 1C), 53.5 (C_s, 1C), 43.5 (C_s, 1C), 43.4 (C_s, 1C), 43.3 (C_q, 1C), 42.9 (C_q, 1C), 38.5 (C_s, 1C), 35.8 (C_s, 1C), 34.8 (C_s, 1C), 29.6 (C_s, 1C), 29.5 (C_s, 1C), 21.5 (C_p, 1C; (CO)CH_3), 21.5 ppm (C_p, 1C; (CO)CH_3); MS (ESI, positive ion mode, MeCN): *m*/*z* (%): 973 [*M*+K]$^+$, 957 [*M*+Na]$^+$.

1,1″-Diethyl-5′-(4-iodobenzyloxy)dispiro[piperidine-4,2′-(7,11,21,25-tetraoxacyclopenta[24.2.2.2^{3,6}.2^{12,15}.2^{17,20}]hexatriaconta-3,5,12,14,17,19,26,28,29,31,33,35-dodecaene)-16,4″-piperidine] (18): In an oven-dried Schlenk tube, amide **17** (169 mg, 1.00 equiv, 0.181 mmol) was dissolved in dichloromethane (35 mL). After cooling to 0 °C (ice bath), DIBAL-H (3.62 mL (1 M in hexane), 2.82 g, 20.0 equiv, 3.62 mmol) was added dropwise over a period of 2.5 h. After stirring for a further 1 h at room temperature, the excess DIBAL-H was quenched with $NaHCO_3$ (saturated aqueous solution). The solution was mixed with basic Celite and filtered. The phases were separated and the aqueous layer extracted with dichloromethane. The combined organic layers were washed once with brine, dried with sodium sulfate, filtered, and concentrated. The crude was purified by column chromatography (SiO_2; EtOAc, 5% MeOH, 5% NEt_3) to give diamine **18** as a colorless oil (74%).

R_f = 0.34 (EtOAc, 5% MeOH, 5% NEt_3); ^{1}H NMR (400 MHz, $CDCl_3$, 25 °C, TMS): δ = 7.63 (d, ^3J(H,H) = 8 Hz, 2H; Ar-H), 7.11–7.05 (m, 4H; Ar-H), 6.97 (d, ^3J(H,H) = 8 Hz, 2H; Ar-H), 6.94 (d, ^3J(H,H) = 8 Hz, 2H; Ar-H), 6.74–6.65 (m, 8H; Ar-H), 6.49 (s, 1H; Ar-H), 4.73 (s, 2H; iodobenzene-CH_2O), 4.10–4.00 (m, 8H; ArOCH_2), 2.65–2.25 (m, 16H), 2.23–2.10 (m, 8H), 1.08–0.99 ppm (m, 6H; CH_2CH_3); ^{13}C NMR (101 MHz, $CDCl_3$, 25 °C, TMS): δ = 156.9 (C_q, 1C), 156.8 (C_q, 1C), 156.6 (C_q, 1C), 145.7 (C_q, 1C), 144.2 (C_q, 1C), 139.8 (C_q, 1C), 138.7 (C_q, 1C), 138.6 (C_q,

1C), 137.7 (C_q, 1C), 137.4 (C_t, 2C), 137.3 (C_q, 1C), 129.1 (C_t, 2C), 127.2 (C_t, 2C), 127.1 (C_t, 4C), 118.7 (C_t, 1C), 114.5 (C_t, 4C), 114.4 (C_t, 2C), 114.3 (C_t, 1C), 113.4 (C_t, 1C), 93.0 (C_q, 1C; C-I), 70.4 (C_s, 1C; iodobenzene-CH_2O), 64.9 (C_s, 1C), 63.7 (C_s, 1C), 63.3 (C_s, 1C), 63.2 (C_s, 1C), 52.3 (C_s, 1C), 49.9 (C_s, 2C), 42.8 (C_s, 1C), 42.7 (C_s, 1C), 42.1 (C_q, 1C), 42.0 (C_q, 1C), 38.5 (C_s, 1C), 29.8 (C_s, 1C), 29.7 (C_s, 1C), 29.6 (C_s, 1C), 29.4 (C_s, 1C), 11.8 ppm (C_p, 2C; CH_2CH_3); MS (ESI, positive ion mode, MeCN): *m/z* (%): 929 $[M+Na]^+$, 907 $[M+H]^+$; HRMS (ESI): *m/z* calcd for $[C_{51}H_{59}IN_2O_5+H]^+$: 907.3541; found: 907.3541.

1,1″-Diethyl-5′-{4-[4-(phenylethynyl)phenylethynyl]benzyloxy}dispiro[piperidine-4,2′-(7,11,21,25-tetraoxacyclopenta[24.2.2.2^{3,6}.2^{12,15}.2^{17,20}]hexatriaconta-3,5,12,14,17,19,26,28,29,31,33,35-dodecaene)-16,4″-piperidine] (23): Bis(dibenzylideneacetone)palladium (3.81 mg, 10 mol%, 6.62 mmol), triphenylphosphine (13.0 mg, 0.750 equiv, 49.6 mmol), and CuI (2.52 mg, 20 mol%, 13.2 mmol) were placed in a preheated 25 mL Schlenk tube. The tube was evacuated and backfilled with argon once. Then a solution of cyclophane **18** (60.0 mg, 1.00 equiv, 66.2 mmol) in THF (crown-cap; 2 mL) and diisopropylamine (DIPA; 2 mL) was added. The resulting suspension was degassed with argon for 10 min. Afterwards, OPE **22** (20.1 mg, 1.50 equiv, 99.3 mmol) was added in one portion and the resulting reaction mixture was stirred at room temperature for 3 h. The reaction mixture was poured into water and extracted three times with EtOAc (30 mL each). The combined organic layers were washed with water and brine, dried with sodium sulfate, filtered, and concentrated. The crude was purified by column chromatography (SiO_2; dichloromethane, 5% MeOH, 1% NEt_3) to obtain compound **23** as a white powder.

R_f=0.42 (EtOAc, 5% MeOH, 5% NEt_3); m.p. 137°C; ^{1}H NMR (400 MHz, $CDCl_3$, 25°C, TMS): δ=7.60–7.50 (m, 6H; Ar-H(OPE)), 7.43 (d, ^3J(H,H)=8 Hz, 2H; Ar-H), 7.38–7.33 (m, 3H; Ar-H(OPE)), 7.16–7.06 (m, 6H; Ar-H), 6.91 (d, ^3J(H,H)=8 Hz, 2H; Ar-H), 6.77–6.63 (m, 8H; Ar-H), 6.47 (s, 1H; Ar-H), 4.85 (s, 2H; $ArCH_2OAr$), 4.13–3.97 (m, 8H; $ArOCH_2$), 2.57–2.25 (m, 16H), 2.24–2.03 (m, 8H), 1.07–1.00 ppm (m, 6H; CH_2CH_3); ^{13}C NMR (101 MHz, $CDCl_3$, 25°C, TMS): δ=156.8 (C_q, 1C), 156.7 (C_q, 1C), 156.7 (C_q, 1C), 147.3 (C_q, 1C), 147.1 (C_q, 1C), 138.2 (C_q, 2C), 131.7 (C_t, 1C), 131.6 (C_t, 2C), 131.6 (C_t, 2C), 131.6 (C_t, 2C), 128.5 (C_q, 2C), 128.4 (C_t, 2C), 127.0 (C_t, 4C), 123.2 (C_q, 2C), 123.0 (C_q, 2C), 122.1 (C_q, 1C), 114.4 (C_t, 2C), 114.3 (C_t, 1C), 91.4 (C_q, 1C; C≡C), 91.3 (C_q, 1C; C≡C), 89.4 (C_q, 1C; C≡C), 89.1 (C_q, 1C; C≡C), 70.6 (C_s, 1C; ArCH_2O), 63.4 (C_s, 1C), 63.2 (C_s, 1C), 63.0 (C_s, 1C), 53.0 (C_q, 1C), 52.4 (C_s, 2C), 50.0 (C_s, 1C), 50.0 (C_s, 1C), 46.2 (C_s, 4C), 43.0 (C_q, 1C), 42.7 (C_s, 1C), 35.1 (C_s, 1C), 35.0 (C_s, 1C), 29.6 (C_s, 1C), 29.5 (C_s, 1C), 12.1 (C_p, 1C; CH_2CH_3), 12.0 ppm (C_p, 1C; CH_2CH_3); MS (ESI, positive ion mode, MeCN): *m/z* (%): 1003 $[M+Na]^+$, 981 $[M+H]^+$; elemental analysis calcd (%) for $C_{67}H_{68}N_2O_5$: C 82.01, H 6.98, N 2.85; found: C 81.58, H 7.34, N 2.87.

1,1,1″1″-Tetraethyl-5′-{4-[4-(phenylethynyl)phenylethynyl]benzyloxy}dispiro[piperidine-4,2′-(7,11,21,25-tetraoxacyclopenta[24.2.2.2^{3,6}.2^{12,15}.2^{17,20}]-hexatriaconta-3,5,12,14,17,19,26,28,29,31,33,35-dodecaene)-16,4″-piperidine] (1): Freshly distilled iodoethane (1.70 mL) was added to the diamine **23** (40 mg, 1.00 equiv, 40.8 μmol). Dry dichloromethane (1 mL) was added to dissolve all of the starting material. The mixture was stirred at room temperature in the dark for 18 h. Then, further dichloromethane (2 mL) was added to suspend the precipitate. After stirring for 5 d at room temperature, the solvent was removed and the crude purified by column chromatography (SiO_2 saturated with 12% methanolic NaBr, dichloromethane, 5% MeOH, then 10% MeOH). The pale-yellow solid obtained was taken up with water and eluted through an ion-exchange column (DOWEX 1X8, 200–400 mesh, Cl^-, packed with water, washed with eluent) eluting with MeCN:H_2O (1:1). The yellow powder obtained was again taken up in water and the precipitate was filtered off. The pale-yellow solid was recrystallized from MeOH/Et_2O (1:1) to obtain the desired amphiphile **1** as a grey solid (59%).

R_f=0.12 (SiO_2, rinsed with 6% (w/v) NaBr in MeOH, CH_2Cl_2, 5% MeOH); ^{1}H NMR (400 MHz, [D_4]MeOH, 25°C, TMS): δ=7.63–7.57 (m, 2H; Ar-H), 7.57–7.49 (m, 4H; Ar-H), 7.41–7.35 (m, 5H; Ar-H), 7.23–7.13 (m, 4H; Ar-H), 7.05–6.94 (m, 5H; Ar-H), 6.92–6.82 (m, 3H; Ar-H), 6.81–6.73 (m, 4H; Ar-H), 6.35 (s, 1H; Ar-H), 4.70 (s, 2H; $ArCH_2OAr$), 4.19–4.03 (m, 8H; $ArOCH_2$), 3.44–3.15 (m, 16H), 2.79–2.48 (m, 8H), 2.23–2.05 (m, 4H), 1.32–1.14 ppm (m, 12H; CH_2CH_3); MS (ESI, positive ion mode, MeCN): *m/z* (%): 519 $[M-2Cl^-]^{2+}$, 512 $[M-Me-2Cl^-]^{2+}$, 505 $[M-Et-2Cl^-]^{2+}$.

Acknowledgements

The authors acknowledge financial support from the Swiss National Science Foundation and the National Center of Competence in Research 'Nanoscale Science'. We also thank Gino Günzburger, Silas Götz, and Gregor Meier for their synthetic support during their laboratory course. Part of this work was supported by the Karlsruhe Nano Micro Facility (KNMF), Helmholtz Research Infrastructure at the Karlsruhe Institute of Technology (KIT). Michel Rickhaus is acknowledged for his beautiful artwork.

[1] F. J. M. Hoeben, P. Jonkheijm, E. W. Meijer, A. P. H. J. Schenning, *Chem. Rev.* **2005**, *105*, 1491–1546.
[2] X. I. Ambroggio, B. Kuhlman, *Curr. Opin. Struct. Biol.* **2006**, *16*, 525–530.
[3] S. Rimmer, I. Soutar, L. Swanson, *Polym. Int.* **2009**, *58*, 273–278.
[4] J. Rotzler, D. Vonlanthen, A. Barsella, A. Boeglin, A. Fort, M. Mayor, *Eur. J. Org. Chem.* **2010**, 1096–1110.
[5] D. Vonlanthen, A. Mishchenko, M. Elbing, M. Neuburger, T. Wandlowski, M. Mayor, *Angew. Chem.* **2009**, *121*, 9048–9052; *Angew. Chem. Int. Ed.* **2009**, *48*, 8886–8890.
[6] D. Vonlanthen, J. Rotzler, M. Neuburger, M. Mayor, *Eur. J. Org. Chem.* **2010**, 120–133.
[7] D. Vonlanthen, A. Rudnev, A. Mishchenko, A. Käslin, J. Rotzler, M. Neuburger, T. Wandlowski, M. Mayor, *Chem. Eur. J.* **2011**, *17*, 7236–7250.
[8] G. W. Gokel, W. M. Leevy, M. E. Weber, *Chem. Rev.* **2004**, *104*, 2723–2750.
[9] D. Gust, T. A. Moore, A. L. Moore, *Chem. Commun.* **2006**, 1169–1178.
[10] C. Renner, L. Moroder, *ChemBioChem* **2006**, *7*, 868–878.
[11] B. L. Feringa, *J. Org. Chem.* **2007**, *72*, 6635–6652.
[12] M. Fujiki in *Amplification of Chirality* (Ed.: K. Soai), Springer, Berlin, Heidelberg, **2007**, p. 119–186.
[13] P. M. Mendes, A. H. Flood, J. F. Stoddart, *Appl. Phys. A* **2005**, *80*, 1197–1209.
[14] B. J. Briscoe, S. K. Sinha, *Materialwiss. Werkstofftech.* **2003**, *34*, 989–1002.
[15] A. G. MacDiarmid, *Angew. Chem.* **2001**, *113*, 2649–2659; *Angew. Chem. Int. Ed.* **2001**, *40*, 2581–2590.
[16] C. Li, H. Bai, G. Shi, *Chem. Soc. Rev.* **2009**, *38*, 2397–2409.
[17] C. R. Crick, I. P. Parkin, *Chem. Eur. J.* **2010**, *16*, 3568–3588.
[18] D. C. Sherrington, K. A. Taskinen, *Chem. Soc. Rev.* **2001**, *30*, 83–93.
[19] D. S. Lawrence, T. Jiang, M. Levett, *Chem. Rev.* **1995**, *95*, 2229–2260.
[20] L. Fang, M. Hmadeh, J. Wu, M. A. Olson, J. M. Spruell, A. Trabolsi, Y.-W. Yang, M. Elhabiri, A.-M. Albrecht-Gary, F. J. Stoddart, *J. Am. Chem. Soc.* **2009**, *131*, 7126–7134.
[21] A. Müller, H. Reuter, S. Dillinger, *Angew. Chem.* **1995**, *107*, 2505–2539; *Angew. Chem. Int. Ed. Engl.* **1995**, *34*, 2328–2361.
[22] D. Bassani, *Nature* **2011**, *480*, 326–327.
[23] M. C. T. Fyfe, F. J. Stoddart, *Acc. Chem. Res.* **1997**, *30*, 393–401.
[24] X. Y. Ling, Y. Xing, D. N. Reinhoudt, J. Huskens, *Pure Appl. Chem.* **2009**, *81*, 2225–2233.
[25] C. J. Pedersen, *J. Am. Chem. Soc.* **1967**, *89*, 7017–7036.
[26] J. Rotzler, M. Mayor, *Chem. Soc. Rev.* **2013**, *42*, 44–62.
[27] L. Fang, M. A. Olson, D. Benítez, E. Tkatchouk, W. A. Goddard III, J. F. Stoddart, *Chem. Soc. Rev.* **2010**, *39*, 17–29.
[28] S. J. Cantrill, G. J. Youn, F. J. Stoddart, D. J. Williams, *J. Org. Chem.* **2001**, *66*, 6857–6872.
[29] M. Zhang, S. Li, S. Dong, J. Chen, B. Zheng, F. Huang, *Macromolecules* **2011**, *44*, 9629–9634.

[30] K.-J. Chang, Y.-J. An, H. Uh, K.-S. Jeong, *J. Org. Chem.* **2004**, *69*, 6556–6563.
[31] R. Hoogenboom, D. Fournier, U. S. Schubert, *Chem. Commun.* **2008**, 155–162.
[32] S.-H. Ueng, S.-Y. Hsueh, C.-C. Lai, Y.-H. Liu, S.-M. Peng, S.-H. Chiu, *Chem. Commun.* **2008**, 817–819.
[33] D. G. Amirsakis, A. M. Elizarov, M. A. Garcia-Garibay, P. T. Glink, F. J. Stoddart, A. J. P. White, D. J. Williams, *Angew. Chem.* **2003**, *115*, 1158–1164; *Angew. Chem. Int. Ed.* **2003**, *42*, 1126–1132.
[34] S. McAlpine, M. A. Garcia-Garibay, *J. Am. Chem. Soc.* **1998**, *120*, 4269–4275.
[35] Z. Fan, Y. Zhao, Y. Liu, *Chin. Sci. Bull.* **2003**, *48*, 1535–1538.
[36] F. Diederich, K. Dick, D. Griebel, *Chem. Ber.* **1985**, *118*, 3588–3619.
[37] F. Diederich, *Angew. Chem.* **1988**, *100*, 372–396; *Angew. Chem. Int. Ed. Engl.* **1988**, *27*, 362–386.
[38] S. W. Tam-Chang, L. Jimenez, F. Diederich, *Helv. Chim. Acta* **1993**, *76*, 2616–2639.
[39] P. Mattei, F. Diederich, *Helv. Chim. Acta* **1997**, *80*, 1555–1588.
[40] T. Marti, B. R. Peterson, A. Fürer, T. Mordasini-Denti, J. Zarske, B. Jaun, F. Diederich, V. Gramlich, *Helv. Chim. Acta* **1998**, *81*, 109–144.
[41] Y. Liu, Z. Fan, H.-Y. Zhang, Y.-W. Yang, F. Ding, S.-X. Liu, X. Wu, T. Wada, Y. Inoue, *J. Org. Chem.* **2003**, *68*, 8345–8352.
[42] N. M. Jenny, M. Mayor, T. R. Eaton, *Eur. J. Org. Chem.* **2011**, 4965–4983.
[43] L. Testaferri, M. Tiecco, M. Tingoli, D. Chianelli, M. Montanucci, *Synthesis* **1983**, 751–755.
[44] C. J. Yu, Y. Chong, J. F. Kayyem, M. Gozin, *J. Org. Chem.* **1999**, *64*, 2070–2079.
[45] L. H. Bluhm, T. Li, *Tetrahedron Lett.* **1998**, *39*, 3623–3626.
[46] X. Huang, Y. Han, Y. Wang, Y. Wang, *J. Phys. Chem. B* **2007**, *111*, 12439–12446.
[47] B. O. Persson, T. Drakenberg, B. Lindman, *J. Phys. Chem.* **1976**, *80*, 2124–2125.
[48] T. W. Davey, W. A. Ducker, A. R. Hayman, *Langmuir* **2000**, *16*, 2430–2435.
[49] R. Margalit, N. Shaklai, S. Cohen, *Biochem. J.* **1983**, *209*, 547–552.
[50] D. Delmarre, N. Hioka, R. Boch, E. Sternberg, D. Dolphin, *Can. J. Chem.* **2001**, *79*, 1068–1074.
[51] S. Anderson, R. T. Aplin, T. D. W. Claridge, T. Goodson II, A. C. Maciel, G. Rumbles, J. F. Ryan, H. L. Anderson, *J. Chem. Soc. Perkin Trans. 1* **1998**, 2383–2398.
[52] D. H. Wu, A. D. Chen, C. S. Johnson, *J. Magn. Reson. A* **1995**, *115*, 260–264.
[53] M. Holz, H. Weingartner, *J. Magn. Reson. (1969)* **1991**, *92*, 115–125.
[54] *TOPSPIN 3.0*, Bruker Biospin GmbH, Software Dept., Rheinstetten, Germany.

Received: July 13, 2012
Revised: October 9, 2012
Published online: January 7, 2013

